

Hanbury-Brown–Twiss signature for clustered substructures probing primordial inhomogeneity in hot and dense QCD matter

Kenji Fukushima,^{1,*} Yoshimasa Hidaka^{2,3,1,4,5,†} Katsuya Inoue^{6,7,8,‡} Kenta Shigaki^{9,7,10,§} and Yorito Yamaguchi^{9,10,||}

¹*Department of Physics, The University of Tokyo, 7-3-1 Hongo, Bunkyo-ku, Tokyo 113-0033, Japan*

²*KEK Theory Center, Tsukuba 305-0801, Japan*

³*Graduate Institute for Advanced Studies, SOKENDAI, Tsukuba 305-0801, Japan*

⁴*International Center for Quantum-field Measurement Systems for Studies of the Universe and Particles (QUP), KEK, Tsukuba 305-0801, Japan*

⁵*RIKEN iTHEMS, RIKEN, Wako 351-0198, Japan*

⁶*Chemistry Program, Hiroshima University, Higashi-Hiroshima, Hiroshima 739-8526, Japan*

⁷*International Institute for Sustainability with Knotted Chiral Meta Matter (SKCM²), Hiroshima University, Higashi-Hiroshima, Hiroshima 739-8526, Japan*

⁸*Chirality Research Center (CResCent), Hiroshima University, Higashi-Hiroshima, Hiroshima 739-8530, Japan*

⁹*Physics Program, Hiroshima University, Higashi-Hiroshima 739-8526, Japan*

¹⁰*Core of Research for the Energetic Universe (CORE-U), Hiroshima University, Higashi-Hiroshima, Hiroshima 739-8526, Japan*



(Received 25 July 2023; revised 11 March 2024; accepted 16 April 2024; published 7 May 2024)

We propose a novel approach to probe primordial inhomogeneity in hot and dense matter which could be realized in noncentral heavy-ion collisions. Although the Hanbury Brown and Twiss (HBT) interferometry is commonly used to infer the system size, the cluster size should be detected if substructures emerge in space. We demonstrate that a signal peak in the HBT two-particle correlation stands at the relative momentum corresponding to the spatial scale of pseudo one-dimensional modulation. We assess detectability using the data prepared by an event generator (AMPT model) with clustering implemented in the particle distribution.

DOI: [10.1103/PhysRevC.109.L051903](https://doi.org/10.1103/PhysRevC.109.L051903)

Introduction. It is an unsettled problem in nuclear physics to explore the phases of matter out of quarks and gluons. The underlying microscopic theory for nuclear dynamics has been established in the form of non-Abelian gauge theory called quantum chromodynamics (QCD). The boundaries of QCD phases in a plane of the temperature T and the baryon chemical potential μ_B constitute the QCD phase diagram; see Refs. [1–4] for reviews. As long as $\mu_B/T \lesssim 2$ is satisfied, the numerical Monte Carlo simulation of lattice-discretized QCD (i.e., lattice QCD) provides us with reliable predictions from the first-principles approach [5]. For $\mu_B/T \gtrsim 2$, however, the sign problem hinders the Monte Carlo algorithm and it still remains a major challenge to unveil the QCD phase diagram in cold and dense regions. There are a variety of speculative scenarios including the QCD critical point, a family

of color-superconducting states, quarkyonic matter [6], dual chiral density waves [7], and inhomogeneous solitonic states [8]. In particular, some states among them hint at a certain shape of spatial modulation. We stress that such modulation or inhomogeneity is not bizarre. The idea of inhomogeneous nuclear matter can be traced back to the old speculation for the p -wave pion condensation [9].

If such exotic scenarios are confirmed in nuclear experiments, it would excite wide interest beyond the nuclear community. It has been known, however, that inhomogeneous phases in three spatial dimensions in the mean-field level are fragile against fluctuations [10,11] and only one-dimensional (1D) quasi-long-range order is expected [12,13]. It has been suggested that the rotonlike dispersion relation appears as a precursory phenomenon of quasi-long-range order at high enough density (called the moat regime) and the characteristic dispersion leads to a possible experimental signature [14]. We note that a stronger argument against inhomogeneous states was given in the mean-field level in a recent study [15]. It is still an open question whether inhomogeneous states could exist in cold and dense nuclear/quark matter. Nevertheless, it is conceivable that clustered substructures may persist as a remnant which we refer to as the *primordial inhomogeneity* with the help of strong magnetic field that effectively reduces the system to a pseudo-one-dimensional state in which the genuine inhomogeneity rather than the quasi-long-range order can develop.

*fuku@nt.phys.s.u-tokyo.ac.jp

†hidaka@post.kek.jp

‡kxi@hiroshima-u.ac.jp

§shigaki@hiroshima-u.ac.jp

||yorito@hiroshima-u.ac.jp

Published by the American Physical Society under the terms of the [Creative Commons Attribution 4.0 International](https://creativecommons.org/licenses/by/4.0/) license. Further distribution of this work must maintain attribution to the author(s) and the published article's title, journal citation, and DOI. Funded by SCOAP³.

Now, a question is the experimental signature for the clustered substructures. We show that the Hanbury Brown and Twiss (HBT) interferometry [16] can resolve the length scale in the particle distribution. For a HBT related idea in the moat regime, see Ref. [17]. The HBT effect is widely known as the quantum interference between identical particles. In nuclear experiments, it is utilized to infer the source size of particle emission via the measured particle correlation functions including the expanding effects [18–21]. In the early days in relativistic heavy-ion collision physics, enhanced pion interferometry radii were discussed as a possible consequence from a first-order phase transition from a quark-gluon plasma to the hadronic phase [22–24]. The so-called ‘‘HBT puzzle,’’ a counterintuitive relation between the sideward and the outward radii, with a naïve expectation with a finite time duration of particle emission, has been intensively discussed to be resolved [25]. Recently, the technique is also applied to femtoscopic correlation measurements to extract hadronic interactions [26,27]. It is important to note that, strictly speaking, the length scale inferred from the HBT correlation is not necessarily the size of the whole system and the cluster size should be more relevant. This is usually taken as a caveat, but for our purpose to seek for inhomogeneity, the cluster size is exactly what we pursue.

Primordial inhomogeneity. The inhomogeneous state is not robust in three spatial dimensions, but the dimensional reduction would justify the one-dimensional (1D) modulation. The well-known example is the superconductivity for which the phase-space integral is effectively 1D near the Fermi surface. In the QCD context, the 1D nature at high baryon density has been discussed in the large number of colors [28–31], and the resulting inhomogeneous phase is called the quarkyonic chiral spirals [30,31].

The dimensional reduction is further assisted by external parameters. In the early stage in the heavy-ion collision, the energy scale of the generated magnetic field, \sqrt{eB} , reaches a scale greater than the typical QCD scale, Λ_{QCD} (or the pion mass m_π), as simulated in Refs. [32,33], and the transverse motion of quarks is frozen. Finite-density QCD matter under strong B develops helical inhomogeneity [34], where the explicit breaking of rotational symmetry due to the magnetic field overrides the realization of quasi-long-range order. In general the lack of rotational symmetry may lead to inhomogeneous states.

More interestingly, the low-energy effective theory of QCD under strong B can be mapped to a model for the chiral magnet [35]. Therefore, the QCD phase structures can be quantitatively deduced from the phase diagram of the chiral magnet. In this way, an analog of the chiral soliton lattice (CSL) is expected for $\mu_B eB / (12\pi^2 f_\pi^2 m_\pi) > 4/\pi$ [36–38]. The QCD CSL state may exist in deep cores of the neutron star and in transient matter created in the noncentral (realizing strong B) heavy-ion collision at intermediate energy (realizing high density). It is pointed out that the rotation velocity ω also favors the QCD CSL state [39].

Let us discuss the primordial inhomogeneity. Figure 1 is a schematic phase diagram with an additional axis of B or ω that favors QCD CSL matter. In low-energy collisions the life time of the magnetic field is significantly enhanced, and the system

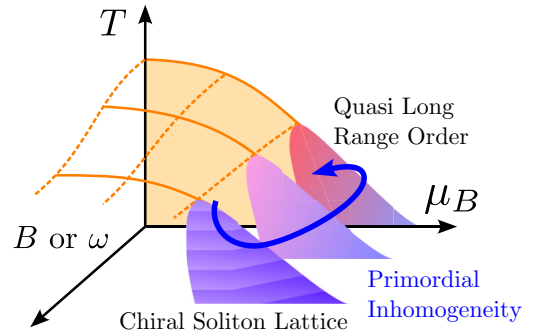


FIG. 1. Schematic illustration for realization of the primordial inhomogeneity as an extension from the QCD CSL state.

may transiently undergo the CSL state. Then, the system expands, as indicated by the arrowed curve, toward a smaller- B and dense regime where the quasi-long-range order is the true ground state. Yet, if the system evolves sufficiently quickly, it may well be trapped in a metastable CSL-like state, which is a mechanism to realize the primordial inhomogeneity.

The discovery of the QCD CSL state would be an intriguing challenge that connects mathematical physics to phenomenology. In dimensionally reduced QCD the vacuum manifold is characterized by $U(1)_L \times U(1)_R / U(1)_V$, which implies that the baryon number appears from the topological winding from the fundamental homotopy group, $\pi_1(S^1)$, while the baryon number arises from the $\pi_3(S^3)$ winding. This mathematical consideration gives feedback to phenomenology: the 1D layered sheets of the π^0 condensate form the domain walls and the baryon number must be localized on them. Therefore, as illustrated in Fig. 2, we can expect CSL-like pseudo-1D modulation along the y axis (which is perpendicular to the reaction plane and parallel to B). Then, π^0 's and baryons could distribute in space with layered substructures. We note that π^\pm are completely suppressed in the infinitely strong- B limit. In reality, however, the modulated π^0 is always accompanied by π^\pm at the edges of the domain walls [38]. So, we focus on the HBT measurement for the $\pi^+-\pi^+$ correlation which is cleaner than the π^0 measurement. We need to consider the effect of the Coulomb interaction, but the Coulomb effect is easily convoluted (or subtracted from the experimental data) with the exact solution of the phase shift. Therefore, assuming that the Coulomb effect is to be canceled, we present our numerical results without any Coulomb interaction.

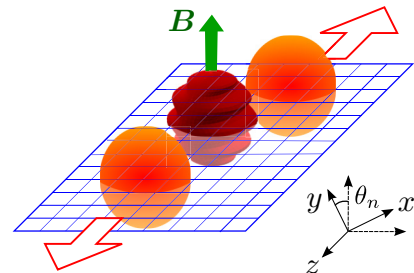


FIG. 2. Collision geometry and the expected pseudo-1D modulation along the magnetic direction in the noncentral collision.

Gaussian analyses. We define the relative momentum and the relative coordinate of two particles as $\mathbf{q} = \mathbf{p}_1 - \mathbf{p}_2$ and $\mathbf{r} = \mathbf{r}_1 - \mathbf{r}_2$. With these variables the two-particle correlation function can be represented as

$$C_2(\mathbf{q}) = \int d^3r S(\mathbf{r}) |\psi_{\text{rel}}(\mathbf{q}, \mathbf{r})|^2 = 1 + \langle \cos(\mathbf{q} \cdot \mathbf{r}) \rangle, \quad (1)$$

where the relative wave function is $\psi_{\text{rel}}(\mathbf{q}, \mathbf{r}) = (e^{-i\mathbf{q} \cdot \mathbf{r}/2} + e^{i\mathbf{q} \cdot \mathbf{r}/2})/\sqrt{2}$, so that its squared quantity is $|\psi_{\text{rel}}(\mathbf{q}, \mathbf{r})|^2 = 1 + \cos(\mathbf{q} \cdot \mathbf{r})$, with the four vectors, \mathbf{q} and \mathbf{r} . Using the on-shell condition, we see that $\mathbf{q} \cdot \mathbf{r}$ is nothing but $-\mathbf{q} \cdot \mathbf{r}$ in the pair rest frame. In our convention $S(\mathbf{r})$ is normalized to satisfy $\int d^3r S(\mathbf{r}) = 1$ and $\langle \dots \rangle$ represents the expectation value weighted by $S(\mathbf{r})$.

For motivating an ansatz for inhomogeneity in $S(\mathbf{r})$, we see a relation between $S(\mathbf{r})$ and the source distribution function $s(\mathbf{r})$. Let us assume a simple source function with 1D spatial modulation (which is along a unit vector \mathbf{n}) parametrized by $s(\mathbf{r}) \propto e^{-r^2/(2r_0^2)} [1 + \tilde{\alpha} \cos(2k\mathbf{n} \cdot \mathbf{r})]$ apart from the normalization. The wave number k characterizes the typical length scale of 1D modulation. Then, if we make only the back-to-back pairs (or we neglect the Lorentz boost effect which turns out to be small), the Gaussian form is simple enough for us to complete the integration of $S(\mathbf{r}) = \int d^3r_1 d^3r_2 s(\mathbf{r}_1) s(\mathbf{r}_2) \delta^{(3)}(\mathbf{r} - \mathbf{r}_1 + \mathbf{r}_2)$ in an analytical way. The result leads us to the following ansatz for the modulated Gaussian:

$$S(\mathbf{r}) = A(\alpha, k, r_0) e^{-r^2/(4r_0^2)} [1 + \alpha \cos(k\mathbf{n} \cdot \mathbf{r})] + O(\alpha^2). \quad (2)$$

Here, $\alpha = 2\tilde{\alpha} e^{-k^2 r_0^2}$ is the amplitude of modulation expressed in terms of parameters in $s(\mathbf{r})$. Parametrically, α is exponentially suppressed for $kr_0 > 1$. This suppression is not a robust feature but a consequence from a simple choice of Gaussian and cosine. Thus, we treat α as a free parameter to be determined by experimental data. The normalization constant is $A(\alpha, k, r_0) = (4\pi r_0^2)^{-3/2} (1 + \alpha e^{-k^2 r_0^2})^{-1}$, with which we find

$$\langle \cos(\mathbf{q} \cdot \mathbf{r}) \rangle = \frac{1 + \alpha e^{-k^2 r_0^2} \cosh(2kqr_0^2)}{1 + \alpha e^{-k^2 r_0^2}} e^{-q^2 r_0^2} \quad (3)$$

for $\mathbf{n} \parallel \mathbf{q}$, which maximizes the modulation effect on the HBT observable. Now that $\mathbf{n} \sim \mathbf{e}_y$, the optimal kinematic condition for the modulation detection is $q_x = q_z = 0$ and we construct $C_2(\mathbf{q})$ as a function of q_y only.

Figure 3 shows the two-particle correlation for the parameter set $r_0 = 6$ fm, $\alpha = 0.6$, and $k = 0.4$ fm $^{-1}$. It is evident that a pronounced peak appears around $k \approx 0.08$ GeV. We note that the typical wave number in the massless CSL is $\mu_B eB / (2\pi f_\pi)^2$ [36], where μ_B is the baryon chemical potential. For eB comparable to $(2\pi f_\pi)^2$, the wave number k should be $\sim \mu_B$. Indeed, an analogous 1D modulation, the chiral spirals, predicts $k \approx 2\mu_B/3$. If we adopt the latter relation, $k = 0.4$ fm $^{-1}$ corresponds to $\mu_B \approx 120$ MeV, i.e., $\sqrt{s_{NN}} \approx 30$ GeV.

The analytical approach is quite useful for the phenomenological implication. The numerical simulation is time-consuming, but we can instantly check the parameter dependence with the obtained analytical solution. For example, it is practically impossible to identify the y axis precisely; in other words, \mathbf{n} may be slightly tilted as $\mathbf{n} \cdot \mathbf{e}_y = \cos \theta_n \neq 1$;

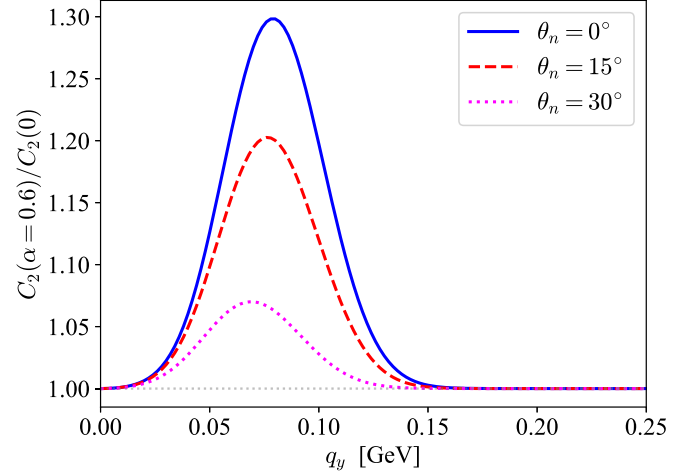


FIG. 3. Normalized two-particle correlation in the simple Gaussian analyses. The system size is chosen to be $r_0 = 6$ fm and the modulation parameters are $\alpha = 0.6$ and $k = 0.4$ fm $^{-1} \simeq 0.08$ GeV. The signal peak stands around $q_y \sim k$.

see the right-bottom corner in Fig. 2. The sensitivity to θ_n is important in practice and, as shown in Fig. 3, the signal peak has strong dependence on θ_n . Also, α might be smaller, but our results imply that, if $\theta_n \approx 30^\circ$ is the experimental bound, only modulations with $\alpha \gtrsim 0.6$ are detectable by about 5% excess in the normalized two-particle correlation.

Phenomenological analyses. The analytical results from the Gaussian formulation are suggestive, but we need to relax the theoretical idealization. In analyzing experimental data, the 1D limit along the y axis cannot be taken. Thus, we must proceed to the model simulation to assess the feasibility. For this purpose, we adopt the AMPT (a multiphase transport) model [40] to simulate the phase-space distribution of produced particles. More specifically, we generated 1000 events of Au-Au collisions at $\sqrt{s_{NN}} = 39$ GeV. The range of the impact parameter is 3.0 fm $\leq b \leq 4.0$ fm for which clustered substructures along the y axis are expected from the pseudo-1D nature. The modulation is introduced by hand, and in this work, all the particles are equally modulated for simplicity. For more systematic surveys, we should focus on particles that couple the baryon number (such as the ω meson), but the analysis simply goes in the same manner (with more statistics required). The particle distribution,

$$\rho(\mathbf{p}, \mathbf{r}, t) = \sum_n \delta(\mathbf{p} - \mathbf{p}_n) \delta(\mathbf{r} - \mathbf{r}_n) \delta(t - t_n), \quad (4)$$

with $(\mathbf{p}_n, \mathbf{r}_n, t_n)$ being the phase-space point of the n th particle emulated by AMPT, is shifted as $\rho[\mathbf{p}, \mathbf{r} - \mathbf{e}_y a \cos(ky), t]$ in our simple ansatz to implement the 1D modulation. The modulation parameter k has the same meaning as our Gaussian approach, and let us choose $k = 0.4$ fm $^{-1}$ again. The amplitude a is not dimensionless and we set $a = 5$ fm in this work. Roughly speaking, the Gaussian model parameter α corresponds to $a \partial_y \rho / \rho$, where $\partial_y \rho / \rho \sim R_y^{-1}$, with R_y being the y length of the system. This parameter of a is the least known part in the whole discussions and should be related to the magnetic strength. In the future, we should proceed to

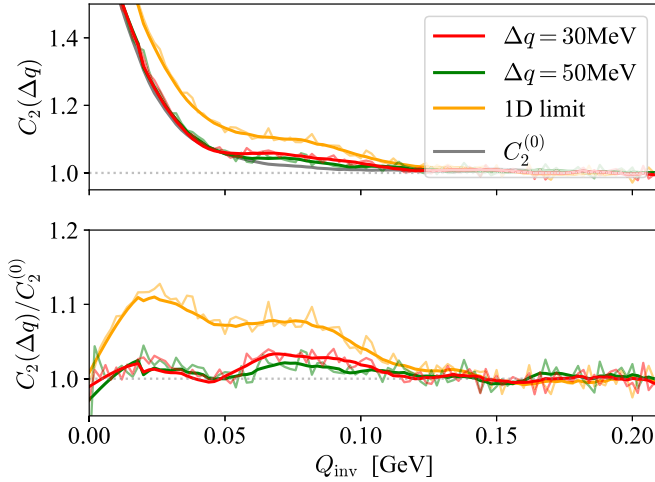


FIG. 4. Two-particle correlation from the AMPT data with the spatial modulation. The tilting angle is fixed as $\theta_n = 20^\circ$. In the upper panel, $C_2^{(0)}$ is the reference, and the lower panel shows the correlation normalized by $C_2^{(0)}$.

systematic investigations. It would be intriguing to determine what a is the sensitivity bound for detectability.

We mention that we mix 1000 events to make pairs. Here, we consider the $\pi^+\pi^+$ pairs and there are 416 824 π^+ 's from 1000 events (with the preselection of $p_z < 1$ GeV). Therefore, one event produces ≈ 400 π^+ 's. If we make pairs within each event, $\approx 8 \times 10^7$ pairs are possible from 1000 events. Since we mix 1000 events, the number of possible pairs is $\approx 8 \times 10^{10}$, which effectively corresponds to 1×10^6 events.

For the evaluation of $\langle \cos(\mathbf{q} \cdot \mathbf{r}) \rangle$ in the transport model calculation, $S(\mathbf{r})$ is approximated into the decomposed form of $s(\mathbf{r}_1)s(\mathbf{r}_2)$. Then, we should make a large number of pairs, i and j , and make $\mathbf{q} = \mathbf{p}_i - \mathbf{p}_j$ and $\mathbf{r} = \mathbf{r}_i - \mathbf{r}_j$ to take the average of $\cos(\mathbf{q} \cdot \mathbf{r})$. We note that the boost effect to the rest frame is included but is negligibly small. The momentum filter is

$$\sqrt{q_x^2 + q_z^2} \leq \Delta q. \quad (5)$$

First, we consider the 1D limit of the analyses. We emulate the 1D limit by computing $\langle \cos(q_y r_y) \rangle$ instead of $\langle \cos(\mathbf{q} \cdot \mathbf{r}) \rangle$ setting $q_x = q_z = 0$. Then, we see a broad bump around 0.08 GeV in Fig. 4, for which we fix $\theta_n = 20^\circ$. For reference, the upper panel of Fig. 4 shows C_2 for $\Delta q = 0.3$ GeV, which is denoted by $C_2^{(0)}$.

The lower panel of Fig. 4 is the ratio to $C_2^{(0)}$, and this quantity serves as a clearer experimental signature. The peak in raw $C_2(\Delta q)$ is washed out for large Δq , but the bump in the ratio remains visible by a few percent (which is experimentally distinguishable) even for $\Delta q = 50$ MeV. In Fig. 4, we present the results for both $\Delta q = 30$ MeV and $\Delta q = 50$ MeV to quantify the dependence on Δq . We have numerically constructed 5×10^5 pairs from 416 824 π^+ 's that satisfy Eq. (5) and taken the average with the 2-MeV bin in terms of $Q_{\text{inv}} = \sqrt{|q^2|}$. Because q_x and q_z are much smaller than q_y , and the boost effect to the pair rest frame is also small, the plots are hardly changed if the horizontal axis is replaced from Q_{inv} to q_y as in Fig. 3. In Fig. 4, the smoothed curves over 20 data points (corresponding to the 40-MeV bin) are overlaid. In this way, we can conclude that the modulation with $a \approx 5$ MeV is well detectable if the experimental accuracy of $\theta_n \approx 20^\circ$ is fulfilled. It should be mentioned that we computed C_2 for $\theta_n = 30^\circ$ and the detectability is marginal. In this way we can make systematic assessment of detectability for a wide variation of parameters, and the present work is the first step along these lines.

Conclusion. We discussed a possibility of clustered substructures in hot and dense matter along the axis parallel to the magnetic field. Even if the magnetic field is short-lived, the pseudo-one-dimensional nature in the early dynamics can induce an inhomogeneous density distribution and the inhomogeneity could remain afterward as a metastable state, which we call the primordial inhomogeneity. We proposed a novel approach to probe the inhomogeneous state using the HBT measurement. Our analytical calculation in the Gaussian formalism exhibits a pronounced peak at the relative momentum corresponding to the wave number of spatial modulation. To assess the feasibility we adopted the phase-space distribution of particles generated by AMPT and computed the two-particle correlation with the spatial substructures of density distribution. We found that the signal excess in the correlation ratio could be suppressed by the alignment of the magnetic axis but still persist under the appropriate momentum filter. Our results are promising enough and the HBT correlations should deserve further systematic investigations.

Acknowledgments. The authors thank Rob Pisarski and Fabian Rennecke for useful correspondences. This work was supported by the Japan Society for the Promotion of Science (JSPS) under KAKENHI Grants No. 22H01216, No. 22H05118 (K.F.), No. 21H01084 (Y.H.), No. 22H02053, No. 25220803 (K.I.), No. 18H05401, and No. 20H00163 (K.S.) and by the JSPS Core-to-Core Program, A. Advanced Research Network.

- [1] K. Fukushima and T. Hatsuda, *Rep. Prog. Phys.* **74**, 014001 (2011).
- [2] K. Fukushima and C. Sasaki, *Prog. Part. Nucl. Phys.* **72**, 99 (2013).
- [3] A. Andronic, P. Braun-Munzinger, K. Redlich, and J. Stachel, *Nature (London)* **561**, 321 (2018).

- [4] C. S. Fischer, *Prog. Part. Nucl. Phys.* **105**, 1 (2019).
- [5] A. Bazavov, H.-T. Ding, P. Hegde, O. Kaczmarek, F. Karsch, E. Laermann *et al.*, *Phys. Rev. D* **95**, 054504 (2017).
- [6] L. McLerran and R. D. Pisarski, *Nucl. Phys. A* **796**, 83 (2007).
- [7] E. Nakano and T. Tatsumi, *Phys. Rev. D* **71**, 114006 (2005).

- [8] M. Buballa and S. Carignano, *Prog. Part. Nucl. Phys.* **81**, 39 (2015).
- [9] A. B. Migdal, *Rev. Mod. Phys.* **50**, 107 (1978).
- [10] L. D. Landau and E. Lifshitz, *Statistical Physics* (Elsevier Science, Amsterdam, 1996).
- [11] R. E. Peierls, *Helv. Phys. Acta* **7**, 81 (1934).
- [12] Y. Hidaka, K. Kamikado, T. Kanazawa, and T. Noumi, *Phys. Rev. D* **92**, 034003 (2015).
- [13] T.-G. Lee, E. Nakano, Y. Tsue, T. Tatsumi, and B. Friman, *Phys. Rev. D* **92**, 034024 (2015).
- [14] R. D. Pisarski and F. Rennecke, *Phys. Rev. Lett.* **127**, 152302 (2021).
- [15] L. Pannullo and M. Winstel, *Phys. Rev. D* **108**, 036011 (2023).
- [16] R. Hanbury Brown and R. Q. Twiss, *Nature (London)* **178**, 1046 (1956).
- [17] F. Rennecke, R. D. Pisarski, and D. H. Rischke, *Phys. Rev. D* **107**, 116011 (2023).
- [18] G. Goldhaber, S. Goldhaber, W.-Y. Lee, and A. Pais, *Phys. Rev.* **120**, 300 (1960).
- [19] B. I. Abelev *et al.* (STAR Collaboration), *Phys. Rev. C* **80**, 024905 (2009).
- [20] A. Adare *et al.* (PHENIX Collaboration), *Phys. Rev. Lett.* **112**, 222301 (2014).
- [21] K. Aamodt *et al.* (ALICE Collaboration), *Phys. Lett. B* **696**, 328 (2011).
- [22] S. Pratt, *Phys. Rev. D* **33**, 1314 (1986).
- [23] G. Bertsch, M. Gong, and M. Tohyama, *Phys. Rev. C* **37**, 1896 (1988).
- [24] D. H. Rischke and M. Gyulassy, *Nucl. Phys. A* **608**, 479 (1996).
- [25] S. Pratt, *Phys. Rev. Lett.* **102**, 232301 (2009).
- [26] L. Adamczyk *et al.* (STAR Collaboration), *Phys. Rev. Lett.* **114**, 022301 (2015).
- [27] Alice Collaboration, *Nature (London)* **588**, 232 (2020); **590**, E13 (2021).
- [28] D. V. Deryagin, D. Y. Grigoriev, and V. A. Rubakov, *Int. J. Mod. Phys. A* **07**, 659 (1992).
- [29] E. Shuster and D. T. Son, *Nucl. Phys. B* **573**, 434 (2000).
- [30] T. Kojo, Y. Hidaka, L. McLerran, and R. D. Pisarski, *Nucl. Phys. A* **843**, 37 (2010).
- [31] T. Kojo, Y. Hidaka, K. Fukushima, L. D. McLerran, and R. D. Pisarski, *Nucl. Phys. A* **875**, 94 (2012).
- [32] V. Skokov, A. Y. Illarionov, and V. Toneev, *Int. J. Mod. Phys. A* **24**, 5925 (2009).
- [33] W.-T. Deng and X.-G. Huang, *Phys. Rev. C* **85**, 044907 (2012).
- [34] G. Başar, G. V. Dunne, and D. E. Kharzeev, *Phys. Rev. Lett.* **104**, 232301 (2010).
- [35] J.-i. Kishine, K. Inoue, and Y. Yoshida, *Prog. Theor. Phys. Suppl.* **159**, 82 (2005).
- [36] T. Brauner and N. Yamamoto, *J. High Energy Phys.* **04** (2017) 132.
- [37] T. Brauner, H. Kolešová, and N. Yamamoto, *Phys. Lett. B* **823**, 136767 (2021).
- [38] S. Chen, K. Fukushima, and Z. Qiu, *Phys. Rev. D* **105**, L011502 (2022).
- [39] X.-G. Huang, K. Nishimura, and N. Yamamoto, *J. High Energy Phys.* **02** (2018) 069.
- [40] Z.-W. Lin, C. M. Ko, B.-A. Li, B. Zhang, and S. Pal, *Phys. Rev. C* **72**, 064901 (2005).